Formation and post-deposition compression of smooth and processable silicon thin films from nanoparticle suspensions

Noah T. Jafferis[a)] and James C. Sturm

Department of Electrical Engineering, Princeton University, Princeton, New Jersey 08544, USA and Princeton Institute for the Science and Technology of Materials (PRISM), Princeton University, Princeton, New Jersey 08544, USA

We report the formation of smooth and processable silicon thin-films from single-crystal silicon-nanoparticle suspensions. Single-crystal Si-nanoparticles (1–4 nm) are produced and suspended in various solvents. Films deposited from the suspension are mechanically stable and can be patterned and processed upon deposition. Physical compression of the films is presented as a mechanism to reduce porosity and global roughness. These thin-films, ~100 nm thick and deposited from a single droplet, contain significant levels of hydrogen, carbon, and oxygen. Resistivities of the as-deposited films are ~$7 \cdot 10^7$ Ω·cm—comparable to intrinsic nanocrystalline-Si. © *2012 American Institute of Physics*. [http://dx.doi.org/10.1063/1.3697980]

I. INTRODUCTION

Additive patterned processes, such as ink-jet printing, are very attractive because they avoid the need for photolithography and etching of blanket layers, waste less material, and have the ability to cover large, flexible substrates. However, wet printing of semiconductors is currently limited primarily to solution-processable organic/polymer semiconductors, which have low mobility (typically up to ~0.1 cm^2/V·s,[1] with some reports of ~1 cm^2/V·s (Ref. 2)). For comparison, the mobility of amorphous silicon used currently in active matrix liquid crystal displays (AMLCDs) is ~1 cm^2/V·s, and that of crystalline silicon as used for VLSI is ~1000 cm^2/V·s.

Recent work on printing silicon from nanoparticles has shown much promise.[3,4] Härting *et al*.[4] report screen-printed films from relatively large nanoparticles (~70 nm diameter) and show mobilities up to ~0.5 cm^2/V·s in as-deposited films. The nanoparticles have an internal grain structure and are produced by mechanical milling of 0.01–0.03 Ω·cm n-type wafers. However, such large particles would lead to rough films and could preclude thin gate dielectrics. This prior work used gate dielectrics of 5–50 μm. The work of Antoniadis *et al*.,[3] on the other hand, still requires heating in the 300–900 °C range. Other methods for printing silicon[5,6] involve producing printable liquid polysilanes (compounds of Si and H). However, this approach includes the necessity for annealing up to 540 °C to produce an a-Si film[5] (with mobilities of ~10^{-3} cm^2/V·s), and the need for further laser-crystallization to achieve mobilities of ~100 cm^2/V·s. In this work we seek an approach similar to that of Ref. 4, depositing droplets of a suspension of Si-nanoparticles with no post-processing heating steps, but with a goal of smooth and processable thin-films (<200 nm) through the use of much smaller (1–4 nm), single crystal Si-nanoparticles. In addition, we present post-deposition compression as a potential room-temperature alternative to standard annealing.

II. POROUS SILICON: FORMATION AND CHARACTERIZATION

We began by forming porous silicon through an electrochemical etching procedure.[7] A silicon wafer (p-type, 1–10 Ω-cm) is suspended in a beaker of HF$_{49\%}$ (49% in H$_2$O), and a voltage is applied between the wafer (the anode) and a platinum cathode. Because the reaction is dependent on the presence of holes (in the p-type Si wafer), the etching will be faster in regions of higher hole concentration and thus in regions of greater current density. This leads to etching in a semi-random manner (depending on the overall current density, HF concentration, crystal orientation, etc.), resulting in porous silicon. Previous work[7] used a mixture of HF$_{49\%}$ and H$_2$O$_2$ (30% in H$_2$O), with H$_2$O$_2$: HF$_{49\%}$ > 2:1, as this had produced the "best" results (smallest particles, narrowest size distribution, lowest percentage of oxygen-terminated Si-bonds). Adding H$_2$O$_2$ has the effect of oxidizing the silicon, while the HF dissolves this oxide, thus increasing the etching rate. It has been shown that current densities of ~5 mA/cm^2 result in etched silicon structures with a characteristic length scale of a few nanometers,[7] so we used similar densities in this work. The etching lasted for ~1.5 h, and went to a depth of ~5–15 μm (as determined from mass lost after etching and ultrasound). To make good electrical contact to the silicon wafer during etching and improve the reproducibility of results, flat "clips" of area ~4 cm^2 were used to contact the wafer. The silicon wafer was placed perpendicular to the acid surface, with electrical contact made at the exposed end. Because of a resistive voltage drop moving away from the contact, porous silicon with features at the desired scale occurred only in a narrow region (~1–5 mm) of the wafer near the acid surface due to the higher current density there. For high throughput, ~10 wafers were contacted and etched at once. The photoluminescence (PL) spectra of the porous silicon produced were measured under various production conditions (current: ~0.04 – 4 mA/cm^2, voltage: ~0 V – 17 V, and HF$_{49\%}$ to H$_2$O$_2$ ratio: 1:1 – 1:3). The incident light was 254 nm UV. All spectra showed similar forms, with peaks at ~650–750 nm

---

a)Electronic mail: jafferis@princeton.edu.

    111, 064316-1

and FWHM of ∼150 nm (Fig. 1). These results are broadly consistent with past measurements of porous silicon luminescence[8] (peaks in the 500–1000 nm range and FWHM of ∼150 nm). Previous measurments[9–11] predict ∼2–5 nm features for the observed emission wavelengths, which is in reasonable agreement with the TEM images of the nanoparticles we produced from these structures (Fig. 2). For reference, we indicate with lines in Fig. 1 several particles sizes corresponding to measured PL[9–11] (solid lines are from Ref. 9; dashed lines from Ref. 11).

III. SILICON NANOPARTICLES: FORMATION AND CHARACTERIZATION

Single-crystal silicon nanoparticles ranging from 1 nm to 4 nm in diameter were produced as a suspension in acetone or other solvents (such as water) by ultrasonic agitation of the porous silicon wafer in the chosen solvent for ∼60 min. Physical vibration crumbles the porous silicon film into nanoparticles,[12] which then disperse into the solvent. Acetone was primarily used because it evaporates quickly during the later printing step. Production of nanoparticles is maximal for etching current densities of 2 to 10 mA/cm^2 and using only HF$_{49\%}$. Under these conditions (and for ∼50 cm^2 of etched wafer), the total mass of silicon consumed by the production process is ∼30–70 mg per hour of processing (etching and ultrasound), as determined by weighing the silicon wafer before etching and after the ultrasound. The total mass of nanoparticles produced is ∼5–11 mg/h, as determined by weighing printed films. Hence, ∼20% of the consumed silicon is retained as nanoparticles. Assuming an average particle diameter of ∼2 nm, the nanoparticle production rate is ∼5·10^{17} particles per hour.

Luminescence measurements and direct TEM imaging were used to determine the size distribution and verify the crystallinity of the particles. A copper grid with carbon film (for TEM) was dipped into a vial of solution and allowed to dry. TEM images of the nanoparticles show that they are single-crystal, through the presence of lattice fringes,[13] and
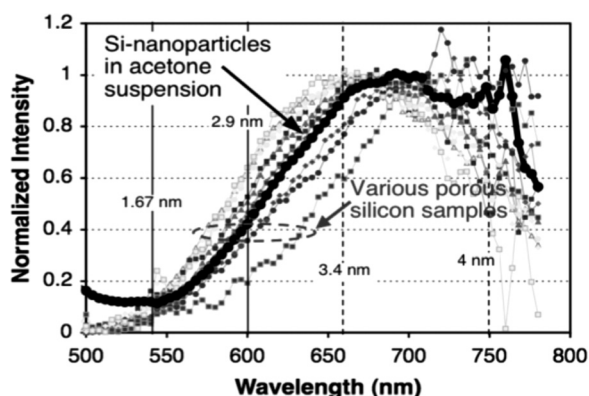
FIG. 1. Luminescence spectra of porous silicon samples producing under various conditions (current: ∼0.04 − 4 mA/cm^2, voltage: ∼0 − 17 V, and HF$_{49\%}$ to H$_2$O$_2$ ratio: 1:1 − 1:3), and luminescence of a vial of nanoparticles suspended in acetone (current: ∼5 mA/cm^2, voltage: ∼15 − 25 V, and HF$_{49\%}$ to H$_2$O$_2$ ratio: 1:3). Lines indicate several particles sizes corresponding to previous PL measurements (solid and dashed lines are from Refs. 9 and 11, respectively).
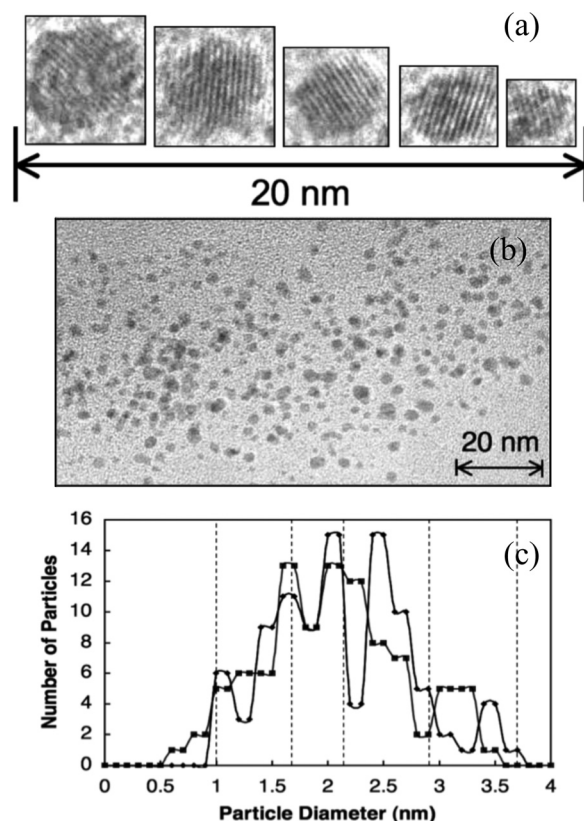
FIG. 2. (a) High-resolution TEM images of several nanoparticles in the 1–4 nm range. The presence of lattice fringes indicates crystallinity. (b) TEM image showing a large number of Si-nanoparticles on a carbon film. (c) Size distribution plot of the nanoparticles. The two plots are for two different TEM grids, but from the same vial of nanoparticles.

range from 1–4 nm in diameter (Fig. 2(a)). The diameters of the particles were measured directly from TEM images (Fig. 2(b)) by drawing two circles on each particle —the largest circle that fit inside, and the smallest circle that contained the particle—and taking the average, leading to the size distribution plot shown in Fig. 2(c). Two different TEM grids for the same solution (etching conditions: current ∼ 3 − 10 mA/cm^2, voltage: ∼30 − 70 V, and HF$_{49\%}$ only) were analyzed. The distributions showed prominent peaks, some of which (e.g., 1.7 and 2.1 nm) were observed on both grids. Discrete peaks in nanoparticle size were observed in a similar work[9]—the vertical lines in Fig. 2(c) indicate the sizes (1, 1.7, 2.15, 2.9, and 3.7 nm) they measured. There is qualitative agreement between these sizes and the peaks in our data, but we did not perform any rigorous statistical analysis. Under 302 nm excitation, luminescence was observed for some of the vials of nanoparticles (when the etching current was ∼3–10 mA/cm^2), with a spectrum quite similar to that observed for the initial porous silicon (Fig. 1). The expected particle sizes (∼2–5 nm) for this spectrum are thus similar to those observed with TEM.

IV. PRINTED THIN-FILMS: FORMATION, CHARACTERIZATION, AND DISCUSSION

Si-nanoparticle thin-films were printed using a syringe to deposit droplets of the nanoparticle suspension onto the desired substrate. For thin film creation, using only HF$_{49\%}$ in

the porous-silicon etching step gives "better" results (smooth, continuous films), perhaps due to a greater volume of nanoparticles produced. Each drop is ∼3.3 μL in volume, and once evaporated, the resultant film is ∼4 mm in diameter. It is desirable to deposit the entire film from only one drop of the suspension—we have produced sufficient quantities of the particles to enable such deposition of thin-films on the order of 100 nm thick. The volume concentration of the nanoparticles in the suspension (C_v) is a critical factor in film production (this is estimated by weighing films printed from a known volume of the suspension). Our experiments indicate that if the concentration is too low ($<1/10\,000$ by volume), only scattered particles or conglomerates of particles will deposit on the substrate (Fig. 3(a)), and a continuous film will not form. On the other hand, if the concentration is too high ($>1/2000$), the film will be greater than ∼300 nm thick, and cracking or peeling will result (Fig. 3(b)). Thus far, only films less than ∼200–300 nm thick have been produced without cracks. Continuous films have successfully been produced for volume fraction concentrations, C_v, of ∼$1.6 \cdot 10^{-4}$ to $3.8 \cdot 10^{-4}$. These films are continuous over the entire area of the deposited droplet (∼0.25 cm^2), with little variation in the thickness. Figures 3(c) and 3(d) show such a film ∼150 nm thick produced from a suspension with $C_v \sim 1.8 \cdot 10^{-4}$.

The films (etching conditions: current ∼ 3 – 10 mA/cm^2, voltage: ∼30 – 70 V, and HF$_{49\%}$ only) were characterized by scanning electron microscopy (SEM) and atomic force microscopy (AFM) to determine thickness and surface roughness, SEM and weighing to determine porosity, and energy dispersive X-ray spectroscopy (EDX) and secondary ion mass spectroscopy (SIMS) to determine composition. Films were deposited on germanium substrates to allow compositional analysis. AFM analysis of the as-deposited films indicate a global roughness of ∼160 nm rms (Fig. 4(a)), which at this scale is dominated by anomalous contamination of large particles on the surface. There was no sign of such clusters or large particles in the TEM data, even at low magnification, so we can conclude that their presence in the printed films is due
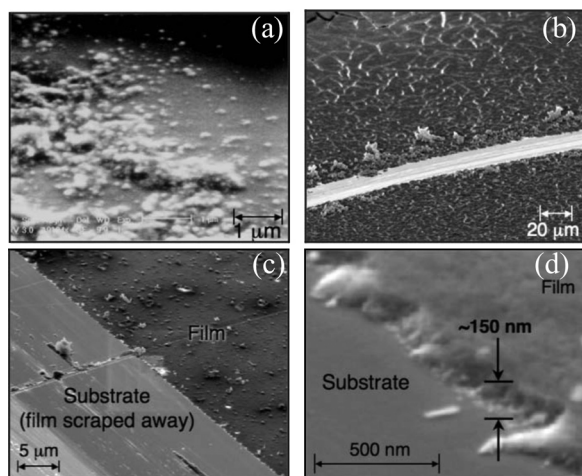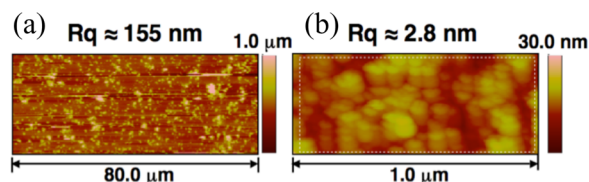

FIG. 4. AFM images showing (a) global roughness (dominated by surface particles) and (b) local roughness (intrinsic film).

either to clustering of smaller particles that occurred only when sufficient numbers of the nanoparticles were deposited (the TEM grid was just briefly dipped in the solution), or to larger particles or clusters in solution which did not stick to the TEM grid. In any case, the local roughness, between the large particles, of ∼3 nm rms (Fig. 4(b)) is indicative of the intrinsic film property. SEM images show pores on the scale of ∼10–50 nm (Fig. 5), which is much larger than the nanoparticle sizes (1–4 nm). By depositing a large number (∼100) of drops on a substrate, a thick enough film (∼10 μm) was formed to measure a difference in the weight of the sample due to the deposited film. This, along with a measurement of the volume of the film, allows the porosity to be estimated at ∼50% to 90%. As a comparison, the porosity that we would obtain if the film were composed of touching spheres would range from 26% for an fcc structure to 48% for a simple cubic structure.

We demonstrate that this high porosity of the film can be reduced by mechanical compression. Using a hard stamp formed from a silicon wafer, with pressures of ∼20–50 psi, we have achieved ∼50% reduction in the thickness of the film, compared to the as-deposited film (Fig. 6). In addition, this compression resulted in a reduction of the global surface roughness (Fig. 6). The inset in Fig. 6 shows that the "pores" seen in the uncompressed region (and in Fig. 5) are no longer visible in the compressed region. Further, the large particles seen in the as-deposited films were no longer present. After stamping, the stamp was inspected in the SEM, and no transfer of material or particles to the stamp was observed. Hence, we conclude that the larger surface particles/clusters have been compressed into the film or broken up by the compression process.

SIMS (Secondary Ion Mass Spectroscopy) analysis of a ∼150-nm film deposited on a germanium substrate (without compression), using acetone as a solvent, confirmed that the

FIG. 3. (a) SEM image showing result of deposition when the nanoparticle concentration (C_v) is less than ∼1/10 000—no continuous film is formed. (b) When the concentration is greater than ∼1/2000, the resultant film is too thick, and cracking occurs. (c), (d) A continuous film ∼150 nm thick produced from a suspension with $C_v \sim 1/5600$.
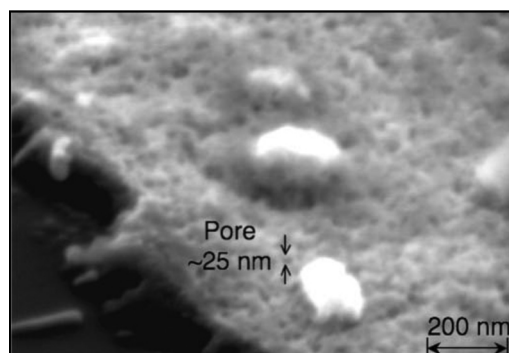

FIG. 5. SEM image showing large surface particles, and also pores in film, as seen by indentations in the surface. Arrows indicate one such pore.
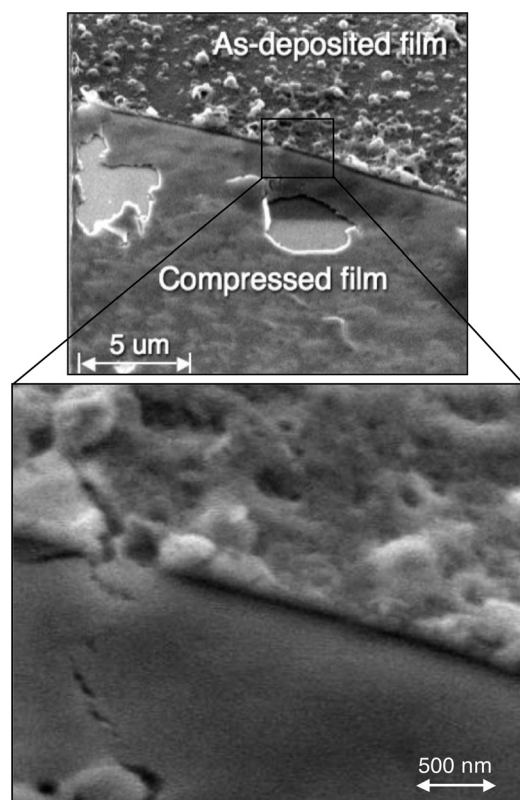
FIG. 6. SEM image of film compression (∼20–50 psi). Inset shows absence of "pores" in compressed area.

FIG. 8. SEM image of the film after patterning to demonstrate its chemical and physical stability. Substrate is SiO_2 on Si.

water-prepared films, the 30 at.% oxygen, along with only ∼3 at.% hydrogen, indicated that the nanoparticles were primarily oxygen-terminated.

To demonstrate chemical and physical stability, films deposited on SiO_2 from the acetone suspensions, even without compression, have been shown to withstand common solvents, photoresist developer, chrome etch, etc. They can be patterned (Fig. 8) using a typical dry (plasma) silicon etch (SF_6/CCl_2F_2: 60/20, 100 mT, 100 W). The etch rate was much slower (∼10–20 nm/min) than the ∼50–100 nm/min expected for nc-Si. Possible causes of the slower etch rate include surface oxide (extends ∼10 nm into the film; Fig. 7) and relatively high oxygen or carbon content within the bulk of the film. Films formed from the water-suspensions were highly non-uniform in thickness and did not continuously cover the substrate. No process patterning or electrical measurements were thus carried out on these samples. Two terminal electrical measurements indicate that the as-deposited acetone-prepared films have dark resistivities of ∼7·10^7 Ω·cm, comparable to that of intrinsic nanocrystalline silicon[14] produced by thermal decomposition of silane onto SiO_2.

V. SUMMARY

Single-crystal silicon nanoparticles (1 to 4 nm in diameter) have successfully been produced and suspended in various solvents by the sonication of porous crystalline silicon. We have demonstrated a process for creating thin films of these silicon nanoparticles by wet printing. The films are mechanically stable and can be patterned and processed, without any temperature treatment after deposition. Thin films ∼100 nm thick have been deposited from a single droplet. They are locally smooth, but highly porous. The porosity and global surface roughness can be significantly reduced by mechanical compression. The films are stable and can be processed and patterned. The measured resistivity of the as-deposited films are ∼7·10^7 Ω·cm, which is comparable to intrinsic nanocrystalline-Si.

ACKNOWLEDGMENTS

deposited film was mostly silicon (Fig. 7). The carbon concentration was ∼10 atomic % throughout the film, while the oxygen level was ∼1 at.% in the bulk of the film. Using water instead of acetone as the solvent did reduce the carbon content to < 1 at.%, but detrimentally increased the oxygen content to over 30 at.%. We conclude that the high carbon content in the acetone-suspension films is due to residual acetone on or between the nanoparticles. The number of hydrogen atoms was nearly the same as that of silicon, which is consistent with the idea that the silicon bonds on the nanoparticles' surfaces are primarily hydrogen-terminated: a 2 nm diameter silicon nanoparticle can be estimated from standard computations to consist of ∼300 silicon atoms. About ∼170 of these would be surface atoms, each able to bond ∼2 hydrogen atoms, on average. For the acetone-prepared films, the number of oxygen atoms in the bulk of the film corresponded to a maximum of 3–6 oxygen atoms per Si-nanoparticle. For the
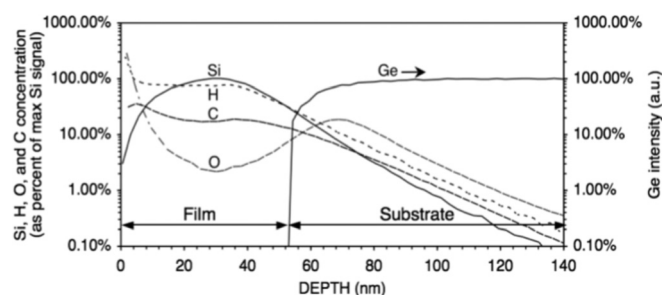

FIG. 7. SIMS analysis of the film. Si-film is on the left side, germanium substrate on the right.
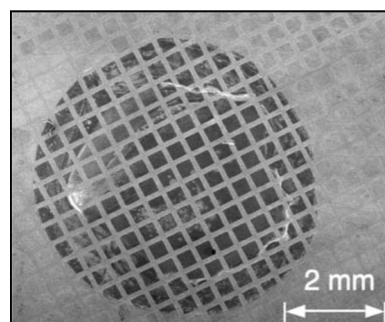
[1] H. Sirringhaus, N. Tessler, and R. H. Friend, Science **280**, 1741–1744 (1998).

[2] S. K. Park, C.-C. Kuo, J. E. Anthony, and T. N. Jackson, Elec. Dev. Meeting, IEEE (2005)

[3] H. Antoniadis, F. Jiang, W. Shan, and Y. Liu, Photovoltaics Specialists Conference (PVSC), 2010, 35th IEEE

[4] M. Härting, J. Zhang, D. R. Gamota, and D. T. Britton, Appl. Phys. Lett. **94**, 193509 (2009).

[5] T. Shimoda, Y. Matsuki, M. Furusawa, T. Aoki, I. Yudasaka, H. Tanaka, H. Iwasawa, D. Wang, M. Miyasaka, and Y. Takeuchi, Nature **440**, 783–786 (2006).

[6] S. Han, X. Dai, P. Loy, J. Lovaasen, J. Huether, J. M. Hoey, A. Wagner, J. Sandstrom, D. Bunzow, O. F. Swenson, I. S. Akhatov, and D. L. Schulz, J. Non-Crystalline Solids **354**, 2623–2626 (2008).

[7] Z. Yamani, W. H. Thompson, L. AbuHassan, and M. H. Nayfeh, Appl. Phys. Lett. **70**, 3404–3406 (1997).

[8] L. T. Canham, in *Properties of Porous Silicon*, edited by L. T. Canham (The Institution of Electrical Engineers, 1997), Chap. 9.1.

[9] G. Belomoin, J. Therrien, A. Smith, S. Rao, R. Twesten, S. Chaieb, M. H. Nayfeh, L. Wagner, and L. Mitas, Appl. Phys. Lett. **80**, 841–843 (2002).

[10] L. Mitas, J. Therrien, R. Twesten, G. Belomoin, and M. H. Nayfeh, Appl. Phys. Lett. **78**, 1918–1920 (2001).

[11] G. Ledoux, O. Guillois, D. Porterat, C. Reynaud, F. Huisken, B. Kohn, and V. Paillard, Phys. Rev. B **62**, 15942 (2000).

[12] O. Akcakir, J. Therrien, G. Belomoin, N. Barry, J. D. Muller, E. Gratton, and M. Nayfeh, Appl. Phys. Lett. **76**, 1857–1859 (2000).

[13] W. Qin and P. Fraundorf, Ultramicroscopy **94**, 245–262 (2003).

[14] J. Y. W. Seto, J. Appl. Phys. **46**, 5247–5254 (1975).